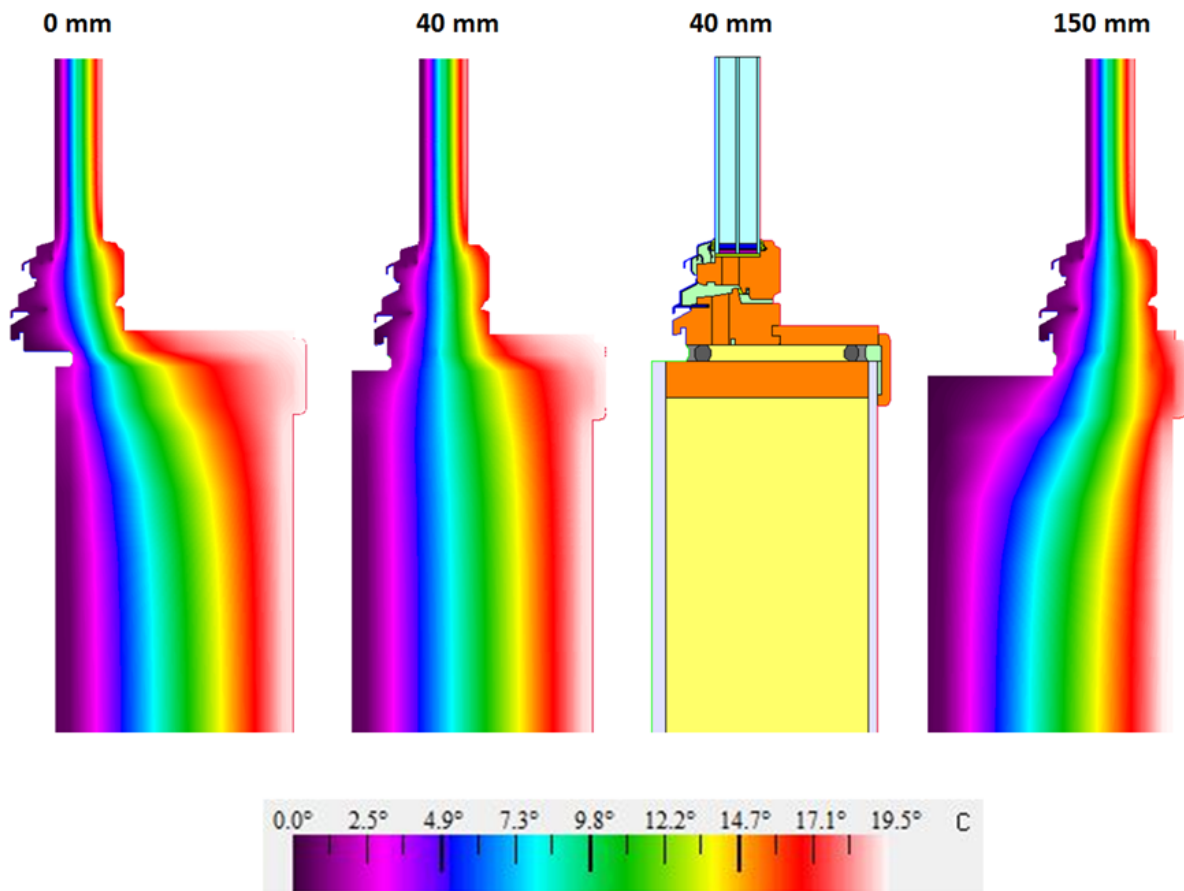


1 The visual summary of the paper:

---



### 3 **Thermal modeling and investigation of the most energy-efficient window position.**

#### 4 *Author names and affiliations:*

5 Cezary Misiópecki, Ph.D. Candidate, Norwegian University of Science and Technology,  
6 Trondheim, Norway

7 Marine Bouquin, Energetic Engineer from ENSGTI (National Engineering School in Industrial  
8 Technologies), Pau, FRANCE

9 Arild Gustavsen, Professor, Norwegian University of Science and Technology, Trondheim,  
10 Norway

11 Bjørn Petter Jelle, Professor, SINTEF Building and Infrastructure / Norwegian University of  
12 Science and Technology, Trondheim, Norway

13

#### 14 ABSTRACT

15 The energy consumption in buildings contributes substantially to the worldwide energy use and  
16 greenhouse gas emissions. One of the crucial elements defining energy consumption is the  
17 building envelope, which in modern designs includes growing share of fenestration. Due to recent  
18 improvements of windows and walls, the thermal bridging effects occurring on their connections,  
19 become more significant. Window-to-wall connections appear to be especially important and  
20 can contribute up to 40% of the total heat loss caused by thermal bridges in building envelope.  
21 Thus, this study is investigating thermal properties of window-to-wall connections. The main  
22 scope of the work is to determine the most optimal window position in the window opening  
23 regarding minimizing thermal bridging effects. Five different wall constructions are investigated  
24 along with two windows with different U-values. The thermal simulation results show that the  
25 window position has a crucial impact on the amount of energy loss through the thermal bridges.  
26 For each wall type, the optimal position is found, resulting from detailed analysis of sill, head,

27 and jambs construction details. For some cases placing the window in the optimal position  
28 reduces linear thermal transmittance (LTT) over 50%. Among considered positions, the  
29 temperatures on the internal surface of the assemblies are weakly influenced by the window  
30 position. Example calculations show that significant share of energy losses from the fenestration  
31 presence is caused by thermal bridge occurring on window-to-wall.

32 **Keywords:** thermal bridge, window-to-wall connection, window position, window opening,  
33 linear thermal transmittance, window U-value, window energy loss.

#### 34 1. INTRODUCTION

35 Saving energy and reducing carbon emissions are currently seen as a worldwide trend. The  
36 buildings energy usage accounts for over 40% of the worlds primary energy use and  
37 approximately 24% of greenhouse gas emissions. This includes direct use of fossil fuels on-site  
38 and indirect use of energy in the form of electricity, district heating, district cooling and the  
39 embodied energy in construction materials [1]. Thus, there is a strong need for reducing the  
40 energy consumption in buildings. One of the crucial elements affecting building energy  
41 consumption is the thermal performance of building envelope. In modern enclosure designs, a  
42 trend of increasing size of fenestration products is noticed. On the one hand, it contributes to a  
43 better living standard by providing more daylight and useful heat gains, but on the other hand, a  
44 higher share of glazed surfaces may also cause higher heat losses or non-desirable heat gains.

45 In recent years due to stricter building codes and further development of low-energy houses,  
46 building envelopes have been substantially improved. Despite that, thermal bridges still occur on  
47 component connection due to their various geometrical shapes or different thermal

48 conductivities. Thermal bridges are causing higher local heat transfer (in comparison to  
49 surrounding structure) thus they significant for the enclosure thermal performance. Higher  
50 thermal resistances of walls, fenestration, roof and slab constructions causing the thermal  
51 bridging effects to become even more pronounced, due to higher share in energy losses [2].  
52 Currently, the thermal transmittance of fenestration products is still significantly higher than for  
53 walls. Among other thermal bridges, the window-to-wall connection appears to be especially  
54 important. The study conducted by Gustavsen et al. [3] shows that for a typical 160 m<sup>2</sup> Norwegian  
55 dwelling, the window-to-wall interface is responsible for about 40% of the total heat loss caused  
56 by thermal bridges. Fairly simple improvements to the connection details for the same case  
57 resulted in 17% reduction of heat losses. Similar outcomes are reported in the international  
58 calculation standard ISO 14683 [4] which describes an evaluation method for thermal bridges.  
59 Calculation for relatively low-performing generic buildings indicates that thermal bridges are  
60 responsible for 36% of the total energy loss through the building envelope, of which 38% is due  
61 to the window-to-wall connection. This demonstrates that the heat loss through the window-to-  
62 wall connection is an important issue in an energy context and should hence not be  
63 underestimated.

64 Methodology for assessing thermal bridges is well established and described in the international  
65 calculation standard ISO 14683. The document also includes universal values of linear thermal  
66 transmittance (LTT) for typical geometric structures occurring in building envelopes, including  
67 window-to-wall connections (refer to ISO14683, Table A2) [4]. Six different simplified wall types  
68 are considered along with three window positions. Typical values of LTT are reported for each  
69 case. The standard indicates preferable window positions in the window openings, however,

70 reported values tend to be much higher than those typical for new construction. Detailed  
71 calculations for individual cases of window-to-wall connections can be conducted according to  
72 ISO 10211 [5] where calculation algorithms are described.

73 The topic of window-to-wall connection has been studied in the literature. Maref et al.  
74 investigated the influence of air leakage on condensation risk [6], [7]. Lacasse et al. presented  
75 solutions reducing water intrusion which could lead to premature failure of the building envelope  
76 [8].

77 First found studies associated with the thermal performance of window-to-wall connections,  
78 were conducted in 2007. In various reports and guidelines, the location of windows in a wall  
79 opening is referred as an important parameter for minimizing effects of thermal bridges. SINTEF  
80 Building Research Project Report no. 25 [3], which focuses on losses caused by thermal bridges,  
81 gives an example of the relationship between the window position and the linear thermal  
82 transmittance for a wood-framed wall including a 250 mm wide insulation layer. This study shows  
83 that installing the window sill 35 mm towards the inside of the wall (measuring from the wind  
84 barrier) is the most favorable regarding reducing thermal bridging. The results have also shown  
85 that the commonly seen practice of aligning window frame with external cladding results in a 6  
86 to 11 times higher value of LTT.

87 Cappelletti et al. [9] investigated the influence of window installation details for clay block walls.  
88 The study simulated the heat flow through wooden windows installed in two different wall  
89 constructions (a brick wall insulated from the outside, and a brick wall with an insulated cavity)  
90 at three positions: outside, intermediate and inside for each wall design. For each case, the linear

91 thermal transmittance based on external dimensions was calculated according to ISO 10211. It  
92 was found that the window position, installation details and the framing of the window aperture  
93 in the wall had a significant impact on the LTT, which differed up to 70% between presented  
94 cases. Also, the study proposed a methodology to combine the heat transfer via thermal bridging  
95 into the window U-value rating.

96 Our previous studies conducted by Decheva [10], Misiopcecki et al. [11], [12] were focused on  
97 determining and lowering LTT values for various window-to-wall connection cases. However,  
98 these studies only considered the connection of window sill with the wall, while jambs and heads  
99 were not considered. The study confirmed results reported in other studies, i.e., that window  
100 positions have a significant effect on the thermal performance of window-to-wall connections.

101 This study expands work performed earlier and focuses on finding the most efficient window  
102 positions, regarding minimizing thermal bridging effects in window openings. The following five  
103 different walls are investigated: wooden-framed wall with various thicknesses, wall retrofitted  
104 with VIPs, concrete wall insulated from the outside, inside and insulated from both sides. Along  
105 with window sills, connections of window jambs and heads are included in the process of finding  
106 the optimal window position. Smaller distance steps are used for more detailed analysis. Each  
107 case is simulated with two window frames with different U-values to determine the influence of  
108 window performance on the optimal position. Additionally, temperatures on the internal  
109 surfaces are tracked in order to assess the sensitivity of condensation risk due to a particular  
110 window position. The study aims to present LTT values for highly insulating window-to-wall

111 connection assemblies and show the quantitative importance of the assembly details on its  
112 thermal performance.

113 The study does not investigate the air leakage or water drainage abilities of the modeled  
114 solutions. Further research is required in this field to assess proposed positions for applicability  
115 in buildings.

## 116 2. METHODOLOGY AND SIMULATION DESCRIPTION

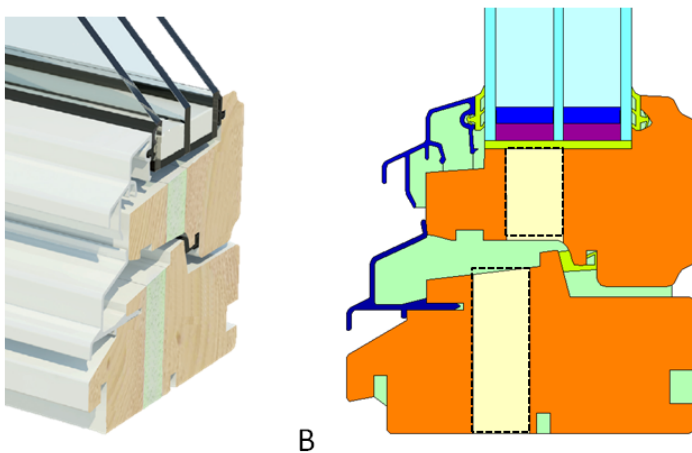
### 117 2.1 Theory

118 Fenestration products interact with other building envelope components. Windows normally  
119 have much lower insulating performance than walls, which creates a thermal bridge on the  
120 components connection. Recent improvements of walls and windows insulating properties  
121 caused the thermal bridge effect to be more significant, due to its relatively higher contribution  
122 to energy losses from the building envelope. Thus, it is important to find the most efficient  
123 window positions for most popular wall constructions which are used in modern construction.

### 124 2.2 Window/frame geometries

125 Thermal simulations are performed using a representative highly performing window product.  
126 The studied window has a wooden frame covered with aluminum on the outside surface.  
127 Moreover, the frame can accommodate polyurethane foam acting as a thermal break which  
128 improves the thermal performance. Both geometries are considered, (i.e., with and without the  
129 thermal break) to investigate the influence of window insulating properties on the optimal  
130 position in the opening. Moreover, the monolithic frame is used along with 2P IGU (double pane

131 insulated glazing unit) incorporating one Low-E coating and argon as a filling gas, which results in  
132 a whole product U-value of  $1.57 \text{ W}/(\text{m}^2\text{K})$ . Thermally broken frame along with 3P IGU (three  
133 panes insulated glazing unit) incorporating two Low-E coatings and krypton as filling gas, provided  
134 a higher performance with U-value of  $0.64 \text{ W}/(\text{m}^2\text{K})$ . Both windows' U-values are assessed  
135 according to the standard ISO 10077-1 [13]. U-values are calculated for products with dimensions  
136 of  $1.23 \text{ m} \times 1.48 \text{ m}$ . Material properties assigned to geometries are obtained from ISO 10077-2  
137 [14]. For the simulations, a simplified version of a high performing, market available spacer is is  
138 used. Figure 1 presents the window sketch and geometry prepared in THERM software.



139

140 **Figure 1 - A: Cross-section drawing of a window used in the study (NorDan 2010), B: Geometry used for thermal modeling using**  
141 **3P IGU. The area marked with dotted lines indicates polyurethane foam.**

### 142 2.3 Selected walls

143 Five different walls constructions are chosen for the simulations. Additionally, wooden-framed  
144 walls and wall retrofitted with VIPs are considered, with 3 and 2 different thicknesses of the  
145 insulation layer, respectively. To simplify the calculations, the same insulation material is used  
146 for each case, with a thermal conductivity of  $0.035 \text{ W}/(\text{mK})$ . Simulated walls are listed and shortly

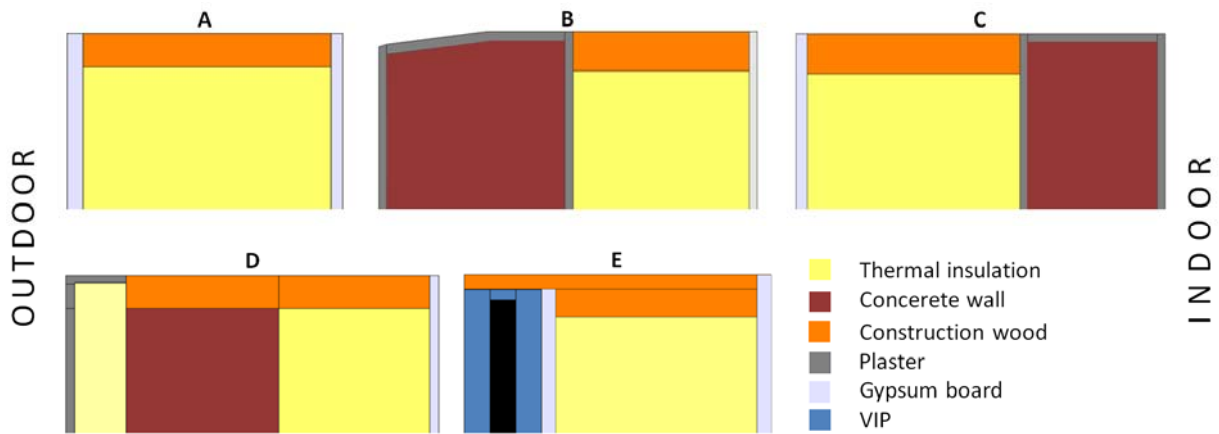


147 described in Table 1. Cross-section drawings of walls are presented in Figure 2. External cladding  
 148 which is typical for walls A and C is not physically modeled, due to simulation simplification.  
 149 Instead, an approach from ISO 6946 [15] is used to account cladding by using a modified  
 150 boundary conditions on the most outside surfaces of the model geometry.

151 **Table 1 – Description of walls selected for the investigation.**

Label	Wall name	Construction	U-value (W/(m <sup>2</sup> K))
A	Wooden-framed wall – 198 mm	Cladding* - Gypsum Board (GB) – insulation layer - GB	0.21
	Wooden-framed wall – 296 mm	Cladding* - GB – insulation layer - GB	0.15
	Wooden-framed wall – 396 mm	Cladding* - GB – insulation layer - GB	0.11
B	Concrete wall insulated from the inside	Plaster - Concrete wall (210 mm) – insulation layer (198 mm) - GB	0.14
C	Concrete wall insulated from the outside	Cladding* - GB - Insulation layer (248 mm) - Concrete wall (160 mm)	0.12
D	Concrete wall insulated from outside and inside	Plaster – Insulation boards (50 mm) – concrete (150 mm) – insulation layer – (148 mm)	0.17
E	Wooden-framed wall (148 mm) retrofitted with VIP	Expanded polystyrene (EPS) (25 mm) – VIP (25 mm) – EPS (25 mm) – GB – insulation layer (148 mm) - GB	0.06
	Wooden-framed wall (198 mm) retrofitted with VIP	EPS (25 mm) – VIP (25 mm) – EPS (25 mm) – GB – insulation layer (198 mm) - GB	0.05

152 \*Cladding has not been physically modeled.



153

154 Figure 2 – Cross-section sketches of walls used in the study. For each wall, the sill is presented. (A) - Wooden-framed wall,  
 155 (B) - concrete wall insulated from the inside, (C) - concrete wall insulated from the outside, (D) - concrete wall insulated from  
 156 outside and inside, (E) - and wooden-framed wall (198 mm) retrofitted with VIP.

## 157 2.4 Numerical simulations

158 Thermal simulations are carried out using the computation program THERM 7.0 which uses the  
 159 finite element method to solve two-dimensional heat conduction governing equation (1) in  
 160 steady state.

$$161 \left( k_{11} \frac{\delta^2 T}{\delta x^2} + k_{22} \frac{\delta^2 T}{\delta y^2} \right) + Q(x, y) = 0 \quad (1)$$

162 where,  $(k_{11})$  and  $(k_{22})$  are conductivities in the x and y directions, respectively,  $(Q)$  - known  
 163 internal heat generation per volume unit. Convection boundary conditions are defined by  
 164 following equation (2):

$$165 q_c = h_c (T_{x,y,z}) * (T - T_c) \quad (2)$$

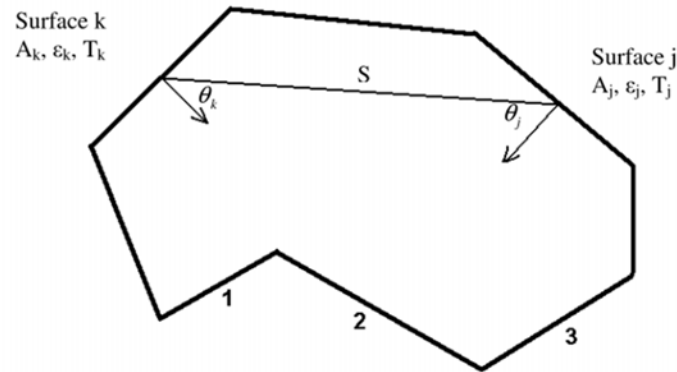
166 where,  $(q_c)$  is convective heat flux,  $(h_c)$  is the convective heat transfer coefficient in the location  
 167 on the boundary  $(x,y,z)$ ,  $(T)$  – temperature and,  $(T_c)$  - reference temperature for convective  
 168 transfer.

169 THERM utilizes CONRAD [16] calculation routine which treats all layers (including air cavities) as  
 170 solids with assigned effective thermal conductivity. Effective conductivity is a sum of gas  
 171 conductivity and convection, radiation mechanisms effects occurring in the air cavity. Convective  
 172 heat transfer is estimated through the use of constant film coefficients which are  
 173 adjusted/assigned depending on cavity geometry, surface temperature, surface emissivity and  
 174 the heat flow direction. Film coefficients built-in software are acquired from experimental studies  
 175 or advanced computational simulations [17], [18]. For more information, please refer to the  
 176 technical documentation describing THERM algorithms [19].

177 Radiation is accounted with the view-factor-based method. The view factor is a fraction of energy  
 178 emitted or reflected from the surface which directly impinges another surface, where is  
 179 absorbed, reflected or transmitted. The view factor is defined by the following equation (3):

$$180 \quad F_{k-j} = \frac{1}{A_k} \iint_{A_k A_j} \frac{\cos\theta_k \cos\theta_j}{\pi S^2} dA_k dA_j \quad (2)$$

181 where,  $S$  is the distance from a point on surface  $A_j$  to a point on surface  $A_k$ ,  $\theta_j$  and  $\theta_k$  are angles  
 182 measured between the line  $S$  and the normal to the surface as shown in Figure 3.



183

184 **Figure 3 - Nomenclature for enclosure radiation [19]**

185

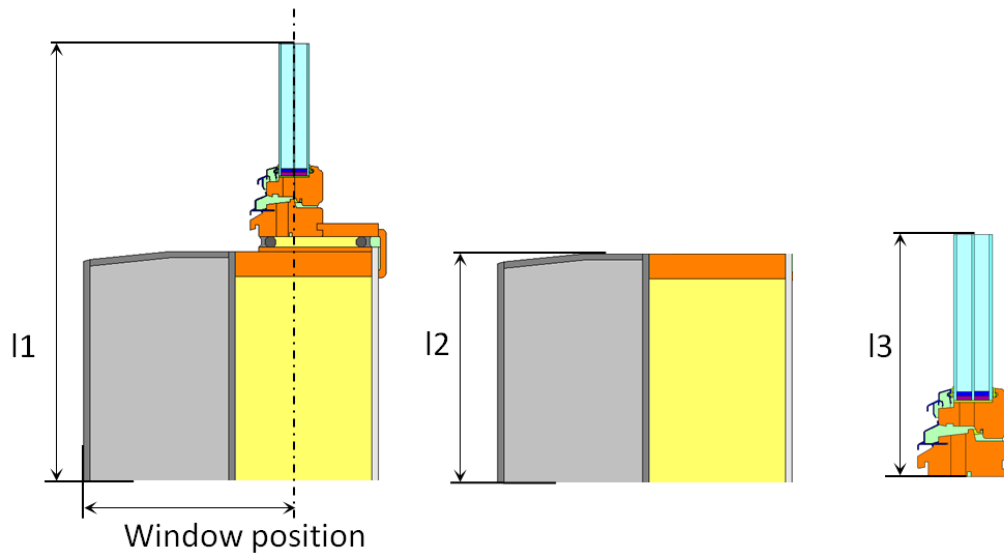
186 The software completing a simulation round checks up solutions for convergence and refines the  
 187 mesh in required areas based on an error-estimation algorithm. The energy error norm for all  
 188 simulations is kept around 6% which yields U-value uncertainty of less than 1% based on THERM  
 189 documentation [19], [20]. The software is used to prepare geometry and conduct heat transfer  
 190 simulations in two-dimensions.

191 Window frame geometry is prepared in accordance with ISO 10077-2 standard and overall  
 192 geometry of window-to-wall connection in accordance with ISO 10211. Boundary conditions for  
 193 the window-to-wall assembly are set as follows. For windows in accordance with ISO 10077-2,  
 194 i.e., indoor/outdoor temperature: 293.15/273.15 K and combined convection and radiation  
 195 coefficient of heat transfer for the indoor/outdoor: 7.692 / 25.0 W/(m<sup>2</sup>K)m respectively. For walls  
 196 in accordance with ISO 6946 where values are the same as for windows, except cases of walls A  
 197 and C for which combined coefficient on the outside side is reduced to 7.692 W/(m<sup>2</sup>K) due to  
 198 established approach of external cladding modeling, which is described the earlier paragraph.

199 Walls are drawn with a height of 1.2 m, and a window is inserted in the various positions. Before  
200 the simulations, international standards were reviewed to find exterior flashing slope for  
201 effective water drainage. In different sources, i.e., ASTM [21] and SINTEF [22], [23] an agreement  
202 on the exterior flashing slope, is not found. It was decided to follow the current SINTEF guidelines  
203 of setting the slope of the sill flashing at ratio 5:1 (horizontal : vertical). If required, for a specific  
204 sill position an additional wooden piece/shim are added to elevate frame and provide a required  
205 slope. Window positions are labeled as a distance from the most outside surface of the wall to  
206 the window symmetry axis. In case of walls A and C, the distance is measured excluding exterior  
207 cladding, starting from the external surface of gypsum board (where alternatively a wind barrier  
208 can be present). An example of geometry and method of indicating window position is shown in  
209 Figure 4. The linear thermal transmittance is calculated according to the following equation (4)  
210 which is derived from ISO14683:

$$211 \quad \psi = L^{2D} - \sum_i U_i \cdot l_i \quad \left[ \frac{W}{mK} \right] \quad (4)$$

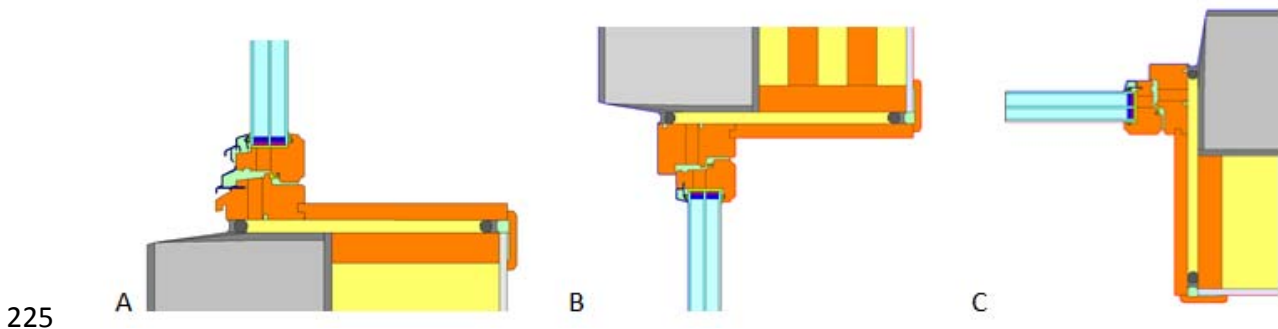
212 where, ( $L^{2D}$ ) is the thermal coupling coefficient obtained from a two-dimensional calculation of  
213 the component separating the two considered environments,  $U_i$  is the thermal transmittance of  
214 the (equivalent) one-dimensional component separating the two considered environments,  $l_i$  is  
215 the length within the two-dimensional geometrical model over which the value of  $U_i$  applies  
216 (refer to Figure 4).



217

218 **Figure 4 - Sketch of example geometry modeled in the study (the model is not to scale).**

219 The geometry of external flashing is not included in the simulation. Pre-simulations indicated that  
 220 it has minor influence both on LTT values and temperature distribution. For the sake of  
 221 simplification, air barriers, tapes, and foils normally used around window openings are not  
 222 included due to their small thickness and limited thermal resistance. All insulation layers are  
 223 modeled as continuous. For each wall, a set of simulations are conducted with several window  
 224 positions in the wall. Each position is evaluated for sill, head, and jambs (refer to Figure 5).



225  
 226 **Figure 5 - Example geometries of window-to-wall for sill (A), head (B) and jambs (C) for concrete wall insulated from the inside,**  
 227 **position 80 mm.**

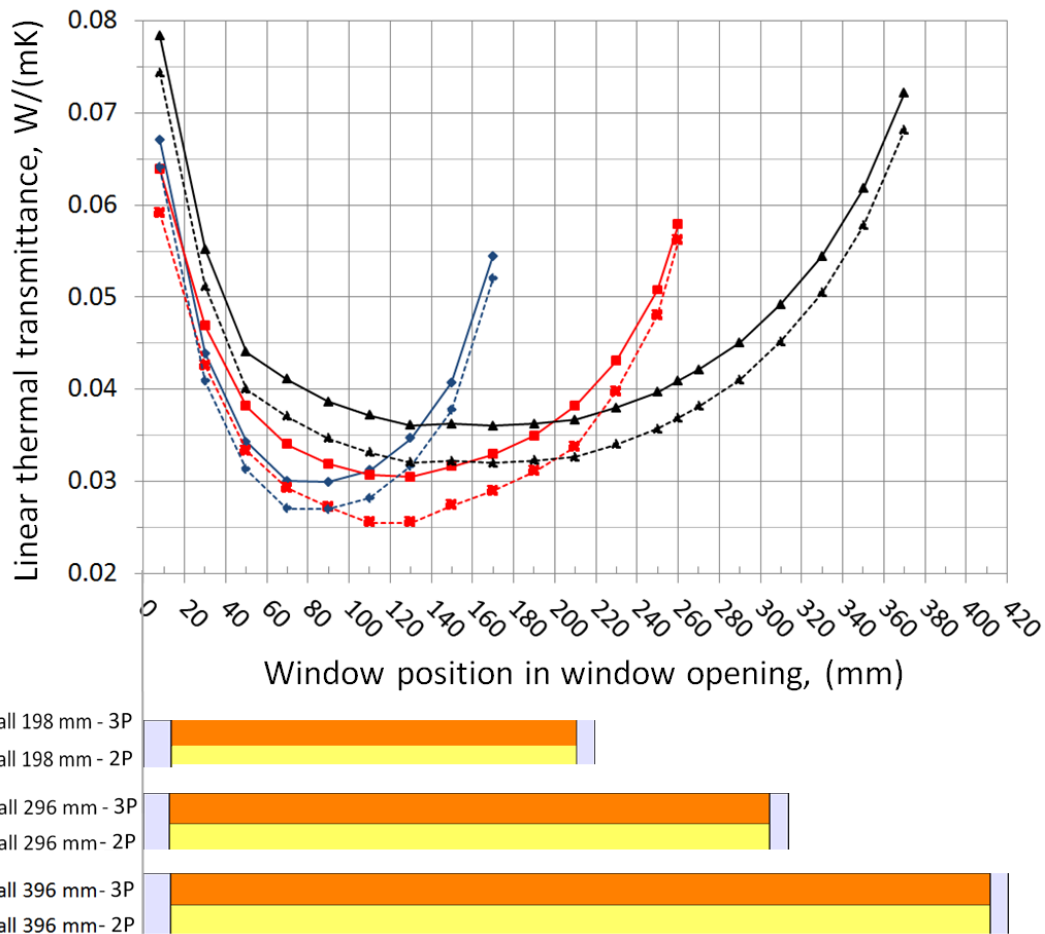
### 228 3. RESULTS AND DISCUSSION

229 Altogether simulations for 660 cases are conducted, and linear thermal transmittance values are  
 230 reported. Due to the high volume of data, the results are presented as graphical plots, which  
 231 show LTT values against window positions. The data is calculated for typical windows with the  
 232 size of 1.23 m x 1.48 m as used in the testing procedure in ISO 12567-1 [24]. Similar graphs were  
 233 also produced for windows with aspect ratios of 2:1 and 1:2. Relatively small differences of LTT  
 234 values are found between jambs and heads, while sills presented a higher discrepancy due to the  
 235 introduction of wooden shims under the frame. However, a maximum actual difference of 0.001  
 236 W/(mK) is found between positions for different aspect ratios, which is around 1% concerning  
 237 the typical LTT values. As an approximation, it can be stated that the presented results are  
 238 representative of most of the typical window units used in buildings.

239 Figure 6 presents results for wooden-framed walls. The LTT values are less sensitive to the  
 240 window position changes and higher for thicker walls. Similar results have also been reported by  
 241 Decheva [10]. Figure 6 presents results for frames incorporating 3P IGU (continuous lines) and 2P

242 IGU (dotted lines). For both windows, construction trends are similar and optimal window  
243 position is the same. In general, low-performing windows with 2P IGU glazing are characterized  
244 by lower values of LTT. For wall construction with insulation layers of 198 mm thickness, the  
245 optimal position is between 70 to 90 mm. For walls including 296 mm and 400 mm insulation,  
246 the most optimal positions are between 90 – 150 and 90 - 230 mm, respectively. For this wall  
247 type, it appears that the most optimal position regarding lowering thermal bridging effect is  
248 approximately in the middle of the wall and some distance towards the outside surface of the  
249 wall. The results revealed that the position of 4 mm (i.e., window outside surface is aligned with  
250 cladding) is not preferable from a thermal point of view. Presented results differ from our earlier  
251 studies since not only the sill is considered and the importance of wooden pieces used for window  
252 elevation is less significant. A temperature difference of 0.4 K is found comparing the lowest  
253 temperature on the internal surface, between the positions.

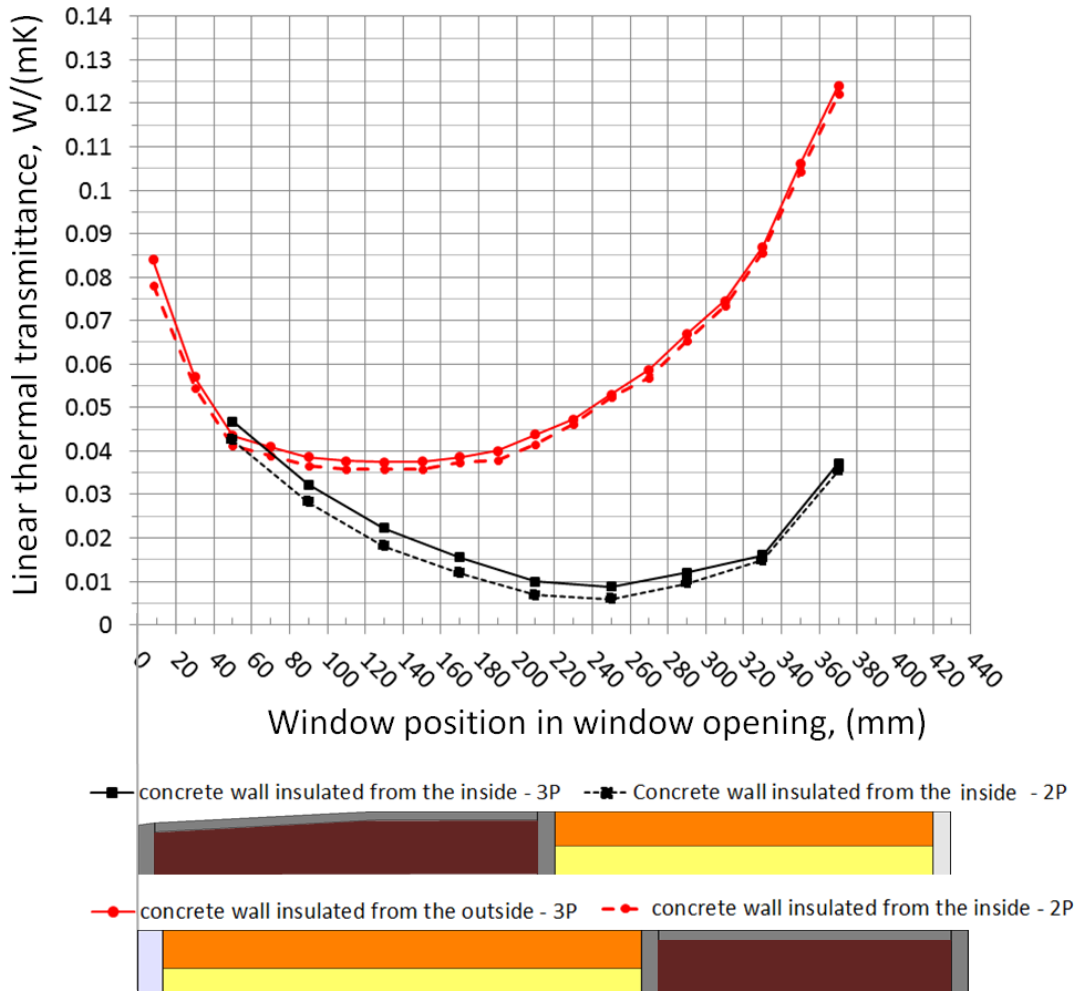




255 Figure 6 – LTT values versus window position in window opening for wooden-framed walls. Colors are indicating materials:  
 256 light grey – gypsum board, orange – construction wood, yellow – insulation.

257 The LTT values for two concrete walls insulated from inside and outside are presented in Figure  
 258 7. Simulations are conducted using two window frames. Again, the window incorporating 2P IGU  
 259 glazing unit has slightly lower LTT values, while trends are almost the same with windows  
 260 including 3P IGU for each wall. For both walls, the position of the window has a significant  
 261 influence on the LTT values. Regarding concrete wall insulated from the outside, a window placed  
 262 in the insulation layer is the most efficient solution. It can be observed that except edges of the  
 263 insulation layer, the thermal bridging effect is weakly sensitive to window position. Similarly to

264 wooden-framed walls, the best values are achieved for positions approximately in the middle of  
 265 the insulation layer and some distance towards the outside wall surface.



266

267 **Figure 7 - LTT values versus window position in window opening for cases of concrete wall insulated from inside and outside.**

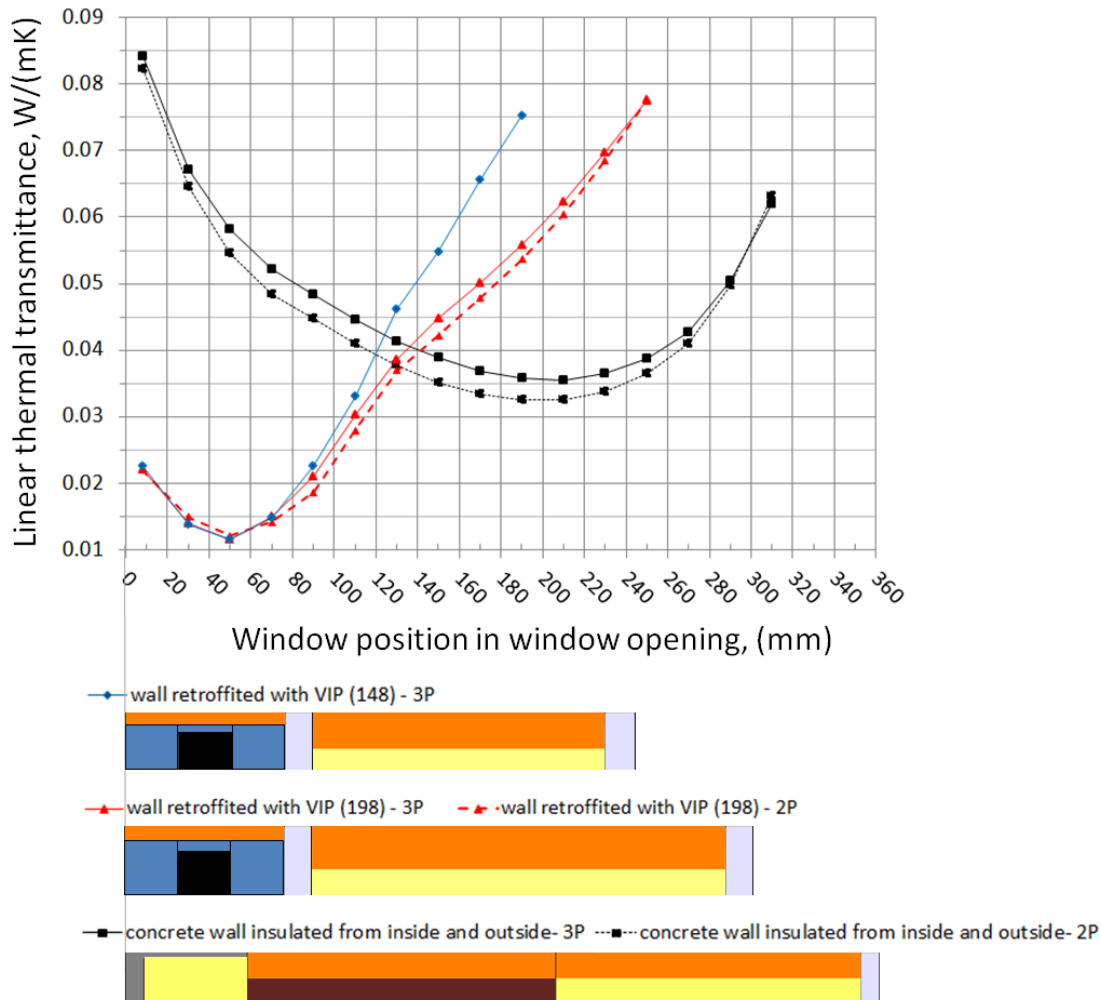
268 **The colors indicate the following materials: light grey – gypsum board, dark grey – plaster, red – concrete, orange- construction**  
 269 **wood, yellow – insulation.**

270 For concrete walls insulated from the inside, a preferable position appears to be at the distance  
 271 of 250 mm. In that position, the window is approximately in-line with the outer surface of the  
 272 insulation. Moving window inside the interval of 200-290 mm provides similar LTT values.

273 Similarly to wooden-framed walls, window position has a minor influence on the internal window  
274 surface temperature, where maximum variation is 0.3 K.

275 Figure 8 presents results for a concrete wall insulated from both sides, and two typical  
276 wooden-framed walls with an insulation layer of 148 and 198 mm retrofitted with encapsulated  
277 VIPs in expanded polystyrene (EPS). Again, two windows are tested for each wall. Similar as for  
278 earlier cases, for the wall with 148 mm thick insulation, LTT values for windows incorporating 2P  
279 and 3P IGU have very similar trends (with slightly lower values for 2P IGU window), thus for  
280 clearer view only results for the 3P IGU window have been shown. For the concrete wall, the  
281 lowest LTT values are achieved for positions in the vicinity of connection between the concrete  
282 wall and the internal insulation layer. Those results are analogic to the concrete wall insulated  
283 from outside. However, the presence of insulation from outside caused a small shift of the  
284 window position towards the outside surface.

285 For typical wooden-framed walls retrofitted with VIPs, the window position is the most sensitive  
286 of all considered walls regarding thermal performance. Results showed that regardless the  
287 thickness of the conventional insulation layer, the preferable window position is just above VIPs.  
288 Maximum differences of lowest temperature on the internal window surface between positions  
289 are found to be 0.5 K.

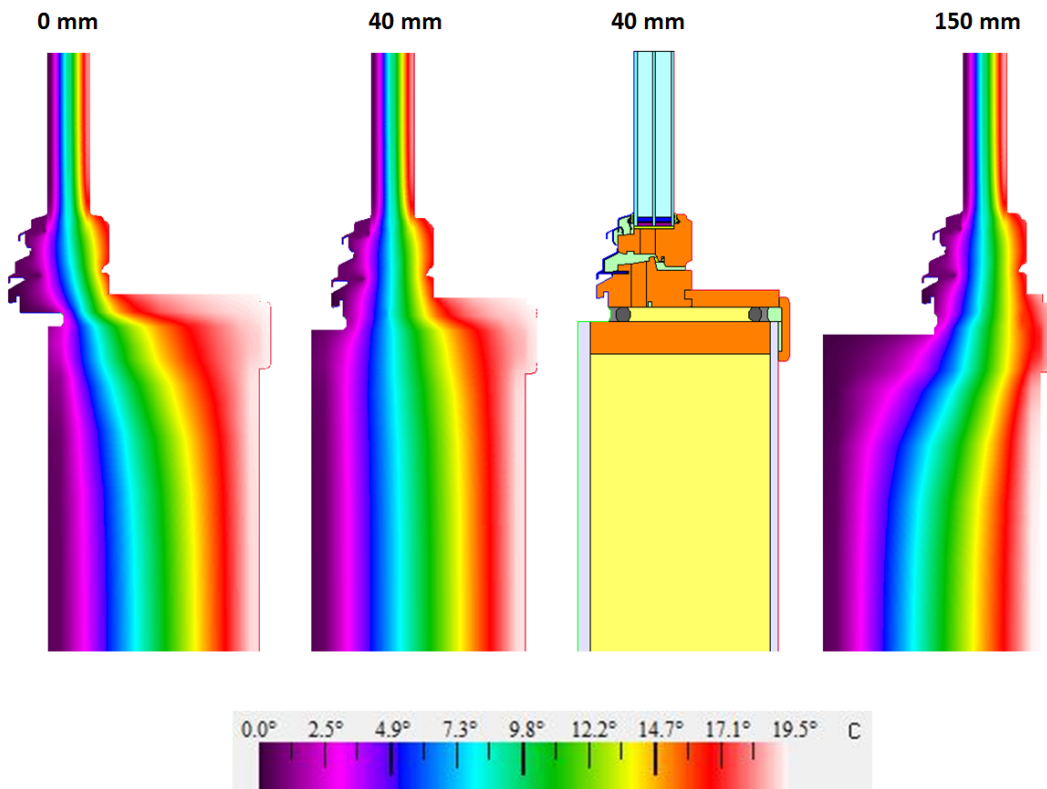


290

291 Figure 8 - LTT values versus window position in window opening for cases of concrete wall insulated from inside and outside  
 292 and walls retrofitted with VIPs. The colors indicate the following materials: light grey – gypsum board, dark grey – plaster, red  
 293 – concrete, orange- construction wood, yellow – insulation, blue – EPS, black - VIP.

294 The presented results indicate the most efficient positions regarding minimizing thermal bridging  
 295 effects on different window-to-wall connections. There may be a few possible reasons why the  
 296 indicated positions show the best insulating properties, which transforms to the lowest LTT  
 297 values. Due to the problem and geometry complexity, it would be difficult to justify the optimal  
 298 position based only on energy governing laws and equations. For better understanding

299 temperature contours are analyzed for different positions. An example temperature contours for  
 300 window positions with high LLT value (8 and 150mm) and optimal position (40mm) in wooden  
 301 framed wall including 198mm of insulation (wall A) are presented in Figure 9.



302

303 **Figure 9 - Temperature contours for frame A (198mm) for different window positions. Additionally, the intersection of**  
 304 **geometry in position (40mm) is added for a better understanding of connection details.**

305 Observations are as following: positions 8 and 150 mm due to window placing have a greater  
 306 heat exchange area on the cold/outdoor side than the window in optimal position. This causes  
 307 higher heat losses of the assembly. Moreover, for both positions 8 and 150 mm isotherms in the  
 308 upper part of the wall are close to each other what indicates higher local temperature gradients  
 309 and effects in higher heat loss.

310 To show the importance of thermal losses from window-to-wall connections which can be related  
311 to window performance, we studied a window (dimensions of 1.23 m x 1.48 m, incorporating 3P  
312 IGU, U-value of 0.64 W/(m<sup>2</sup>K)) inserted in a wooden-framed wall with an insulation thickness of  
313 296 mm. The total heat loss of the window itself equals to 23.30 W (calculated according to the  
314 formula: window U-value x window area x dT; 0.64 W/(m<sup>2</sup>K) x (1.23 m x 1.48 m) x 20K= 23.30 W)  
315 if we assume a temperature difference across the geometry equal to 20 K. For wooden-framed  
316 wall commonly seen in practice is flashing/aligning window surface with the external cladding  
317 (refer to position 4 mm). This position would result in an additional loss (caused by thermal bridge  
318 of window-to-wall connection) of 6.94 W (calculated according to the formula: LTT x perimeter  
319 of the window x dT; 0.064 W/(mK) x (2 x 1.48 m + 2 x 1.23 m) x 20 K = 6.94 W). For optimal  
320 windows position (110 mm) the additional loss equals to 3.36 W (calculated: 0.031 W/(mK) x (2  
321 x 1.48 m + 2 x 1.23 m) x 20 K = 3.36 W). Calculations show that placing windows in the optimal  
322 position reduces losses by 3.58 W which is around 15% of the losses caused by the entire window  
323 itself.

#### 324 4. CONCLUSIONS

325 The study is investigating thermal properties of window-to-wall connections. The main scope is  
326 to determine the most optimal window position in a window opening regarding minimizing a  
327 thermal bridging effect. Five different wall constructions have been investigated along with two  
328 windows with various insulating properties. Results show that the position of the window has a  
329 crucial impact on the thermal bridging effect. Highest and lowest Linear Thermal Transmittance  
330 (LTT) values for the following wall types along with 3P window are: A (198mm): 0.067/0.030 A  
331 (296mm): 0.064/0.030, A (400mm): 0.078/0.036, B: 0.047/0.009, C: 0.084/0.036, D: 0.084/0.037,

332 E(148mm): 0.075/0.011, E(198mm): 0.077/0.011 W/(mK) . For each wall type, the optimal  
333 position is found, considering the connection of the sills, head, and jambs separately. Estimated  
334 linear thermal transmittance (LTT) values for windows with different aspect ratios are very close.  
335 Thus results are applicable for most common window shapes used in the building industry.  
336 Moreover, no significant differences in trends and optimal positions are found between two  
337 tested windows, which may indicate that the window insulating properties have a limited effect  
338 on the optimal position. However, slightly lower LTT values are found for lower thermally  
339 performing windows, i.e., the thermal bridging effect is more important for highly performing  
340 products. Furthermore, the temperature differences on the internal surface of the assemblies  
341 are not significantly affected by the window position (a maximum difference of 0.5 K). It is shown  
342 by a simple calculation using specific geometries that additional heat loss caused by the thermal  
343 bridge on window-to-wall connection is relatively high. Placing a window in the position  
344 according to common practice results in additional loss up to 30% of the entire window heat loss.  
345 By placing a window in the optimal positions, the thermal bridge losses could be reduced by more  
346 than 50%. Thus it is important to design window-to-wall connections carefully.

#### 347 ACKNOWLEDGEMENTS:

348 This work has partly been funded by the Research Council of Norway, Lian Treverefabrikk and  
349 Lawrence Berkeley National Laboratory (LBNL) through the NTNU and SINTEF research project  
350 “Improved Window Technologies for Energy Efficient Buildings” (EffWin), and the Assistant  
351 Secretary for Energy Efficiency and Renewable Energy, Office of Building Technology, Building

352 Technologies Program of the U.S. Department of Energy under Contract no. DE-AC02-  
353 05CH11231.

354 REFERENCES

- 355 [1] K. Voss, E. Musall, IEA-SHC Task 40 / ECBCS Annex 52 || Zero Energy Building | Zero  
356 Emission Building | Net Zero Energy Solar Buildings, (2010). [http://members.iea-  
357 shc.org/task40/](http://members.iea-shc.org/task40/).
- 358 [2] B. Berggren, M. Wall, Calculation of thermal bridges in (Nordic) building envelopes - Risk  
359 of performance failure due to inconsistent use of methodology, *Energy Build.* 65 (2013)  
360 331–339. doi:10.1016/j.enbuild.2013.06.021.
- 361 [3] A. Gustavsen, J.V. Thue, P. Blom, A. Dalehaug, T. Aurlien, S. Grynning, S. Uvsløkk,  
362 Prosjektrapport 25: Kuldebroer – Beregning , kulde- broverdier og innvirkning på  
363 energibruk. (Project report 25: Thermal bridges - calculation, values, impact on energy  
364 use), (2008).
- 365 [4] E. ISO, 14683: Thermal bridges in building construction–Linear thermal transmittance–  
366 Simplified methods and default values., (2007).
- 367 [5] E. ISO, ISO 10211:2007 Thermal bridges in building construction - Heat flows and surface  
368 temperatures - Detailed calculations, (2007).
- 369 [6] W. Maref, N. Van Den Bossche, M. Armstrong, M.A. Lacasse, H. Elmahdy, R. Glazer,  
370 Condensation risk assessment on box windows: the effect of the window–wall interface,  
371 *J. Build. Phys.* 36 (2012) 35–56. doi:10.1177/1744259111411653.
- 372 [7] W. Maref, N. Van De Bossche, M. Armstrong, M.A. Lacasse, H. Elmahdy, R. Glazer, B.S.  
373 Kaskel, R.J. Kudder, M.R. Mitchell, R.E. Link, Laboratory Tests of Window-Wall Interface  
374 Details to Evaluate the Risk of Condensation on Windows, *J. Test. Eval.* 39 (2011) 103071.  
375 doi:10.1520/JTE103071.
- 376 [8] M.A. Lacasse, M. Manning, M. Rousseau, S.M. Cornick, S. Plescia, Results on Assessing the  
377 Effectiveness of Wall-Window Interface Details to Manage Rainwater, (2007).
- 378 [9] F. Cappelletti, A. Gasparella, P. Romagnoni, P. Baggio, Analysis of the influence of  
379 installation thermal bridges on windows performance: The case of clay block walls, *Energy  
380 Build.* 43 (2011) 1435–1442. doi:10.1016/j.enbuild.2011.02.004.
- 381 [10] L.M. Decheva, Vinduer for energieffektive bygninger - Kuldebroer ved vindusinnseting.  
382 (Windows for energy effective buildings - Thermal bridges by window insertion). M.Sc.  
383 thesis, Norwegian University of Science and Technology (NTNU), (2012).
- 384 [11] C. Misiwopecki, A. Gustavsen, W.C. DuPont, J. Kosny, A. Fallahi, N. Shukla, Optimization of  
385 Window Installations in Deep Energy Retrofits Using Vacuum Insulation Panels, in: 2nd  
386 Cent. Eur. Symp. Build. Phys., Vienna, Austria, Europe, 2013.
- 387 [12] C. Misiwopecki, A. Gustavsen, B.P. Jelle, L. Decheva, Practical Methods for Ensuring Energy



- 388 Efficient Window-Wall Connections, in: Build. XII Conf., Clearwater, Florida, US, 2013.
- 389 [13] ISO 10077-1:2006, 10077-1: 2006, Therm. Perform. Wind. Doors Shutters--Calculation  
390 Therm. Transm. 1 (2009).
- 391 [14] ISO, 10077-2: Thermal performance of windows, doors and shutters--Calculation of  
392 thermal transmittance--Part 2: Numerical method for frames (ISO 10077-2: 2003), (2003).
- 393 [15] ISO, ISO 6946: Building components and building elements - Thermal resistance and  
394 thermal transmittance - Calculation method, (2007).
- 395 [16] A. Shapiro, Two-Dimensional Finite Element Code for Heat Transfer Analysis, Electrostatic,  
396 and Magnetostatic Problems, Lawrence Livermore Natl. Lab. Rep. UCID-20824. (1986).
- 397 [17] Y. Zhao, D. Curcija, W.P. Goss, Condensation resistance validation project - detailed  
398 computer simulations using finite-element methods, 1996.
- 399 [18] ASHARE, ASHARE - Handbook of Fundamentals, Chapter 15 - Fenestration., (2009).
- 400 [19] Lawrence Berkeley National Laboratory, Conrad 5 & Viewer 5 Technical and Programming  
401 Documentation, (2006).
- 402 [20] Lawrence Berkeley National Laboratory, THERM / WINDOW - NFRC Simulation Manual,  
403 (2011).
- 404 [21] ASTM, Standard Practice for Installation of Exterior Windows , Doors and Skylights 1,  
405 (2002).
- 406 [22] SINTEF, 523.701 - Innsetting av vindu i vegger av bindingsverk. (Installation of windows in  
407 wooden frame walls), (2003).
- 408 [23] SINTEF, 523.702 - Innsetting av vindu i mur- og betongvegger. (Installation of windows in  
409 brick and concrete walls), (2003).
- 410 [24] ISO, ISO 12567-1:2010 Thermal performance of windows and doors - Determination of  
411 thermal transmittance by the hot-box method - Part 1: Complete windows and doors,  
412 (2010).
- 413